

NATIONAL ADVISORY COMMITTEE FOR AERONAUTICS

TECHNICAL NOTE 4248

SUMMARY OF EXPERIMENTAL HEAT-TRANSFER MEASUREMENTS
IN TURBULENT FLOW FOR A MACH NUMBER
RANGE FROM 0.87 TO 5.05

By Maurice J. Brevoort and Barbara D. Arabian

Langley Aeronautical Laboratory
Langley Field, Va.



Washington
May, 1958

AFMCC

TECHNICAL LIBRARY



TECHNICAL NOTE 4248

SUMMARY OF EXPERIMENTAL HEAT-TRANSFER MEASUREMENTS

IN TURBULENT FLOW FOR A MACH NUMBER

RANGE FROM 0.87 TO 5.05

By Maurice J. Brevoort and Barbara D. Arabian

SUMMARY

Heat-transfer measurements have been made in turbulent flow at Mach numbers varying from 0.87 to 5.05 and Reynolds numbers in the range from 1×10^6 to 9.5×10^8 through the use of an axially symmetric annular nozzle which consists of an inner shaped center body and an outer cylindrical sleeve. Measurements taken along the outer sleeve gave essentially flat-plate results that are free from wall interference and corner effects.

These results are presented in the form of Stanton number and recovery factor as a function of Reynolds number. The Reynolds number is computed for wall and free-stream conditions; that is, the viscosity is taken at either the wall or the free-stream temperature.

The results show that the Stanton number decreases with an increase in Reynolds number and usually decreases with an increase in Mach number. The recovery factor appears from these tests to be independent of Mach number and may be represented by a single curve for all Mach numbers in the range of the tests.

INTRODUCTION

The design of supersonic aircraft and missiles requires engineering information about heat-transfer coefficients and temperature recovery factors for supersonic speeds that extend over a wide range of Reynolds number. In references 1, 2, 3, 4, and 5, local turbulent-heat-transfer measurements were presented for Mach numbers of 3.03, 2.06, 1.62, 0.87, and 3.90, respectively.

The information presented in the present report consists of a summary of the work presented in the previous reports with additional test data from a series of tests at higher Reynolds numbers and at a Mach number of 5.05.

The range of Reynolds numbers for which measurements were obtained is from approximately 1×10^6 to 9.5×10^8 . The highest Reynolds numbers were obtained with the lowest Mach numbers. The difference between wall temperature and equilibrium temperature during the tests varied throughout the tests and to some extent with the Mach number. The data presented in the report were obtained at temperature differences of from 5° to 40° F. The average value of the ratio of inner surface wall temperature to free-stream temperature T_w/T_∞ varied with Mach number, the average values being 1.0, 1.6, 1.8, 3.0, 4.0, and 5.5 for Mach numbers of 0.87, 1.62, 2.06, 3.03, 3.90, and 5.05, respectively.

SYMBOLS

c	specific heat of sleeve material, Btu/lb- $^\circ$ R
c_p	specific heat of air at constant pressure, Btu/lb- $^\circ$ R
g	acceleration due to gravity, ft/sec ²
h	heat-transfer coefficient, Btu/ft ² -sec- $^\circ$ R
k	heat conductivity of wall, Btu/ft-sec- $^\circ$ R
l	wall thickness
M	Mach number
N_{Nu}	Nusselt number, hx/k
N_{St}	Stanton number, $h/\rho V c_p g$
p_o	settling-chamber pressure
R	Reynolds number, $\rho V x/\mu$
T_{av}	average wall temperature, $^\circ$ R
T_e	effective stream air temperature at wall, some temperature which gives a thermal potential which is independent of the heat-transfer coefficient h , $^\circ$ R
T_t	stagnation temperature, $^\circ$ R

T_w	inside-surface temperature of nozzle sleeve, °R
T_∞	free-stream temperature, °R
t	time, sec
V	free-stream velocity, ft/sec
w	specific weight of sleeve material, lb/sq ft of surface exposed to air flow
x	longitudinal distance along sleeve, ft (unless otherwise indicated)
η_r	recovery factor, $\frac{T_e - T_\infty}{T_t - T_\infty}$
μ	dynamic viscosity coefficient, lb-sec/sq ft
ρ	free-stream density of air, slugs/cu ft

APPARATUS AND METHODS

The apparatus consisted of an axially symmetric annular nozzle which was directly connected to the settling chamber of one of the blowdown jets of the Langley gas dynamics laboratory. The nozzle had a center body shaped to give the desired Mach number. Two center-body series were employed, one for 8-inch- and the other for 11-inch-diameter sleeves. The 8-inch sleeves, 41 inches long, were constructed with two wall thicknesses, 0.388 inch of carbon steel and 0.060 inch of stainless steel. The 11-inch sleeve, 80 inches long, was constructed of 0.750-inch-thick carbon steel. The coordinates of both series of center bodies are given in table I.

The sleeve was heavily insulated with glass wool. The effectiveness of this insulation was checked by a few tests made with the sleeve surrounded by a vacuum. The results for these tests were in good agreement with those made under normal testing conditions; accordingly, heat loss by external convection and conduction was not considered significant. Radiation, which leads to a correction of less than 2 percent, was also ignored.

A drawing of the test arrangement is shown in figure 1. In the figure a typical center body is shown in an 8-inch sleeve. Locations of the

thermocouples and the static-pressure orifices are also shown. Figure 2 shows the inlet and center-body support for the 11-inch sleeve. A typical center body is shown in figure 3.

Figure 4 shows the detail of thermocouple installation. The thermocouple junction is located 0.060 inch from the inner surface of the shell. The wires are No. 30 (0.010-inch diameter) copper-constantan wire. Conduction is negligible along the wire. As indicated in figure 4, the thermocouples are in intimate contact with the metal so that thermal resistance at the junction is also negligible.

Figure 5 shows the detail of a static-pressure-orifice installation. By means of these orifices the Mach number was measured along the length of the sleeve and checked at regular intervals around the sleeve. Figure 6 shows the measured Mach number distribution for all nozzles.

The temperature-recording equipment consisted of synchronized high-speed Brown recorders, each having 12 channels. The settling-chamber thermocouple was connected to each recorder for comparison purposes. The stagnation temperature was varied throughout the test to give large heat-transfer rates and both positive and negative ratios. The recorders are accurate to $\pm 1^\circ$ F and are consistent to a value somewhat better than 1° F.

A typical stagnation-temperature variation is presented in figure 7 together with the corresponding wall-temperature variation for station 14. These readings are for the 11-inch nozzle at a Mach number of 3.90 and a settling-chamber pressure of 353 lb/sq in. gage.

Throughout the test the maximum pressures were limited to approximately 500 lb/sq in. The minimum pressures were limited by starting conditions or the limit of accuracy. The first 20 seconds of each test were excluded from the computations because this time was required to stabilize the pressure for the desired operating condition.

In figure 8 values of wall temperature are plotted against longitudinal distance along the cylinder for various times during the test.

These values are needed to evaluate the longitudinal conduction $K \frac{d^2T}{dx^2}$. In order to avoid the effects of longitudinal conduction, values to be used in the final computation of heat transfer were confined to ranges where d^2T/dx^2 approached zero.

REDUCTION OF DATA

The equations used in reducing the data are

$$\eta_r = \frac{T_e - T_\infty}{T_t - T_\infty} \quad (1)$$

$$h = wc \frac{dT_{av}/dt}{T_w - T_e} \quad (2)$$

$$N_{St} = \frac{h}{\rho V c_p g} \quad (3)$$

The method presented herein consists of selecting a recovery factor and then obtaining the value of T_e from equation (1). For each recovery factor that is selected, the corresponding quantity $T_w - T_e$ is determined and then plotted against the heat input $wc \frac{dT_{av}}{dt}$. (See fig. 9.) The curve connecting these points is a straight line (eq. (2)). The true values of T_e and η_r are obtained when the line goes through zero. The slope of this line is the value of h . This method of data reduction is illustrated by figure 9, which shows the values used in determining η_r and h for $M = 3.90$ at station 14 for a settling-chamber pressure of 353 lb/sq in. gage. The Stanton number corresponding to the value of h determined from this figure is calculated from equation (3).

The value of dT_{av}/dt used in equation (2) is that of the actual thermocouple reading, whereas it should be the value associated with the average wall temperature in the thickness of the sleeve at each point. At the beginning of a test it is obvious that the value of dT/dt is too high when the thermocouple is located at the heat-transfer surface and too low when it is located at the insulated surface. The product wc of the sleeve mass per unit area and the specific heat of the wall material is accurate to ± 5 percent.

Under some peculiar conditions of high heat transfer and small temperature differences $T_w - T_e$, it is possible to obtain heat-transfer coefficients or Stanton numbers which have significant errors because

the thermocouple is located at a point inside the shell wall, 0.060 inch from the surface instead of at the heated surface.

Hill (ref. 6) has developed a method for evaluating the heat transfer under transient conditions for thick-walled bodies. When the heat transfer is computed by the methods of reference 6 there is good agreement with the simpler but less accurate method used herein for evaluating the test data. The test at $M = 0.87$ and a settling-chamber pressure of 450 lb/sq in. gage should have the largest error of any of the tests presented herein. The methods of reference 6 were used to obtain the wall temperature from the measured temperature and from this information, the heat transfer and Stanton number. Any deviations in the results computed by reference 6 and the original computations were too small to warrant correcting the final curves.

Figure 10, which is reproduced from reference 1, shows the variation of Nusselt number $\left(N_{Nu} = \frac{hx}{k}\right)$ with Reynolds number. When these data were originally presented in this form, it was noted that the points for each pressure tended to fall on a curve which at the highest values of x appeared to become asymptotic to a straight line.

The x -value used in the computations of these data had been arbitrarily selected as zero at the throat of the nozzle. Selection of this value is equivalent to assuming that the Reynolds number is zero at that point and that this is the transition point or point of initial turbulent boundary layer. Clearly, the transition point tends to move upstream as the stagnation pressure increases. On the basis of this argument, the x -values were adjusted so that all the data fell in a straight line. Further, this adjustment to the values of x was made for all subsequent tests and is noted in the figures.

RESULTS AND DISCUSSION

The final results are presented as curves of the variation of Stanton number with Reynolds number (figs. 11 and 12). The results presented in references 1 to 5 are included in these figures together with additional results at high Reynolds numbers and for a Mach number of 5.05. The Stanton number for each Mach number is presented once for a Reynolds number based on wall conditions (fig. 11) and again for a Reynolds number based on free-stream conditions (fig. 12). Each Reynolds number uses the value of ρv at free-stream conditions but the viscosity is taken in regard to the particular condition of wall or free-stream temperature. In figure 12 the curve calculated by the method of Van Driest (ref. 7) at the test value of T_w/T_∞ is plotted along with a curve faired through datum points from the present tests.

An examination of the test results presented in figure 12 shows that the data for Mach numbers of 3.03 and 3.90 fall somewhat above the Van Driest curve. The considerations outlined in the section entitled "Reduction of Data" may explain the variation. This explanation is especially likely in the case for the Mach number of 3.03 for which the temperature difference $T_w - T_e$ was smaller than in the other tests and thus tended to exaggerate the effect of a small correction to the wall temperature.

Figures 13 and 14 give the recovery factor as a function of Reynolds number for both wall and free-stream conditions. The absence of a systematic variation of recovery factor with Mach number suggests that a single curve might be used for all the test Mach numbers. Such a curve is plotted in figures 13 and 14.

The effect of Mach number on the heat transfer can be demonstrated from the experimental data by comparing Stanton numbers from the tests with the Stanton number for incompressible flow or $M = 0$ (ref. 7). Such a comparison is given in figure 15. In general, there is a decrease in Stanton number with an increase in Mach number and, further, the results for a Mach number of 5.05 appear to have an anomalous variation with Reynolds number. The most likely and simplest explanation is that these results were obtained in the transition region for $M = 5.05$.

CONCLUDING REMARKS

Heat-transfer measurements have been made in turbulent flow at Mach numbers varying from 0.87 to 5.05 and Reynolds numbers in the range from 1×10^6 to 9.5×10^8 through the use of an axially symmetric annular nozzle which consists of an inner shaped center body and an outer cylindrical sleeve. Measurements taken along the outer sleeve gave essentially flat-plate results that are free from wall interference and corner effects.

These results are presented in the form of Stanton number and recovery factor as a function of Reynolds number. The Reynolds number is computed for wall and free-stream conditions; that is, the viscosity is taken at either the wall or the free-stream temperature.

The results show that the Stanton number decreases with an increase in Reynolds number and usually decreases with an increase in Mach number. The recovery factor appears from these tests to be independent of Mach

number and may be represented by a single curve for all Mach numbers in the range of the tests.

Langley Aeronautical Laboratory,
National Advisory Committee for Aeronautics,
Langley Field, Va., February 12, 1958.

REFERENCES

1. Brevoort, Maurice J., and Rashis, Bernard: Turbulent-Heat-Transfer Measurements at a Mach Number of 3.03. NACA TN 3303, 1954.
2. Brevoort, Maurice J., and Rashis, Bernard: Turbulent-Heat-Transfer Measurements at a Mach Number of 2.06. NACA TN 3374, 1955.
3. Brevoort, Maurice J., and Rashis, Bernard: Turbulent-Heat-Transfer Measurements at a Mach Number of 1.62. NACA TN 3461, 1955.
4. Brevoort, Maurice J., and Rashis, Bernard: Turbulent-Heat-Transfer Measurements at a Mach Number of 0.87. NACA TN 3599, 1955.
5. Brevoort, Maurice J.: Turbulent-Heat-Transfer Measurements at a Mach Number of 3.90. NACA TN 3734, 1956.
6. Hill, P. R.: A Method of Computing the Transient Temperature of Thick Walls From Arbitrary Variation of Adiabatic-Wall Temperature and Heat-Transfer Coefficient. NACA TN 4105, 1957.
7. Van Driest, E. R.: The Turbulent Boundary Layer for Compressible Fluids on a Flat Plate With Heat Transfer. Rep. No. AL-997, North American Aviation, Inc., Jan. 27, 1950.

TABLE I.- CENTER-BODY COORDINATES

(a) $M = 0.87$; 8-inch-diameter sleeve

x, in.	Radius, in.
-11.0	2.130
-9.0	2.700
-7.0	3.050
-5.0	3.250
-3.0	3.380
-1.0	3.450
0	3.474
33.5	3.340
36.0	3.383

(b) $M = 0.87$; 11-inch-diameter sleeve

x, in.	Radius, in.
-9.0	2.750
-8.0	2.880
-7.0	3.100
-6.0	3.450
-5.0	3.860
-4.0	4.280
-3.0	4.680
-2.0	5.000
-1.0	5.130
0	5.160
10.0	5.116
20.0	5.073
30.0	5.030
40.0	4.986
50.0	4.942
60.0	4.898
70.0	4.854
72.5	5.018

TABLE I.- CENTER-BODY COORDINATES - Continued

(c) $M = 1.62$; 8-inch-diameter sleeve

x, in.	Radius, in.	x, in.	Radius, in.
-10.00	2.000	1.30	3.3491
-4.70	2.000	1.40	3.3402
-4.50	2.020	1.50	3.3317
-4.00	2.100	1.60	3.3238
-3.00	2.500	1.70	3.3167
-2.50	2.735	1.80	3.3103
-2.00	2.970	1.90	3.3047
-1.50	3.150	2.00	3.2997
-1.00	3.300	2.10	3.2955
-.80	3.340	2.20	3.2920
-.60	3.375	2.30	3.2891
-.40	3.400	2.40	3.2868
-.20	3.425	2.50	3.2851
0	3.4375	2.60	3.2839
.10	3.4364	2.70	3.2831
.20	3.4337	2.80	3.2827
.30	3.4298	2.90	3.2825
.40	3.4249	5.00	3.2720
.50	3.4190	10.00	3.2470
.60	3.4122	15.00	3.2220
.70	3.4045	20.00	3.1970
.80	3.3961	25.00	3.1720
.90	3.3871	30.00	3.1470
1.00	3.3776	35.00	3.1220
1.10	3.3680	38.625	3.1059
1.20	3.3584		

TABLE I.- CENTER-BODY COORDINATES - Continued

(d) $M = 1.62$; 11-inch-diameter sleeve

x, in.	Radius, in.
-9	2.750
-8	2.880
-7	3.100
-6	3.450
-5	3.860
-4	4.280
-3	4.680
-2	5.000
-1	5.220
0	5.3000
.10	5.2979
.20	5.2925
.30	5.2848
.40	5.2756
.50	5.2662
.60	5.2580
.70	5.2516
.80	5.2471
.90	5.2444
1.00	5.2432
1.09	5.2428
5.00	5.179
10.00	5.154
20.00	5.104
30.00	5.054
40.00	5.004
50.00	4.954
60.00	4.904
70.00	4.854

TABLE I.- CENTER-BODY COORDINATES - Continued

(e) $M = 2.06$; 8-inch-diameter sleeve

x, in.	Radius, in.	x, in.	Radius, in.
-10.25	2.000	1.8	3.1787
-4.7	2.000	1.9	3.1618
-4.5	2.020	2.0	3.1456
-4.0	2.100	2.1	3.1303
-3.0	2.500	2.2	3.1157
-2.5	2.735	2.3	3.1020
-2.0	2.970	2.4	3.0890
-1.5	3.150	2.5	3.0769
-1.0	3.300	2.6	3.0655
-.8	3.340	2.7	3.0550
-.6	3.375	2.8	3.0453
-.4	3.400	2.9	3.0364
-.2	3.425	3.0	3.0283
0	3.4375	3.1	3.0211
.1	3.4364	3.2	3.0147
.2	3.4333	3.3	3.0091
.3	3.4280	3.4	3.0043
.4	3.4204	3.5	3.0004
.5	3.4108	3.6	2.9974
.6	3.3990	3.7	2.9952
.7	3.3852	3.8	2.9939
.8	3.3696	3.9	2.9934
.9	3.3522	4.0	2.9924
1.0	3.3336	5.0	2.9824
1.1	3.3141	10.0	2.9324
1.2	3.2941	15.0	2.8824
1.3	3.2739	20.0	2.8324
1.4	3.2538	25.0	2.7824
1.5	3.2341	30.0	2.7324
1.6	3.2149	34.0	2.6924
1.7	3.1964	34.250	2.6999

TABLE I.- CENTER-BODY COORDINATES - Continued

(f) $M = 2.06$; 11-inch-diameter sleeve

x, in.	Radius, in.
-10.25	2.750
-4.0	2.750
-3.5	2.850
-3.0	3.113
-2.5	3.475
-2.0	3.840
-1.5	4.240
-1.0	4.625
-.5	4.888
0	5.0000
.1	4.9990
.2	4.9958
.3	4.9904
.4	4.9830
.5	4.9733
.6	4.9615
.7	4.9477
.8	4.9321
.9	4.9148
1.0	4.8961
1.5	4.7966
2.0	4.7081
2.5	4.6394
3.0	4.5908
4.0	4.5551
5.0	4.5151
10.0	4.4751
20.0	4.3951
30.0	4.3151
40.0	4.2351
50.0	4.1551
60.0	4.0751
70.0	3.9951

TABLE I.- CENTER-BODY COORDINATES - Continued

(g) $M = 3.03$; 8-inch-diameter sleeve

x, in.	Radius, in.
-10.25	2.000
-4.7	2.000
-4.5	2.020
-4.0	2.100
-3.5	2.208
-3.0	2.380
-2.5	2.620
-2.0	2.893
-1.5	3.170
-1.0	3.387
-.8	3.444
-.6	3.482
-.4	3.512
-.2	3.527
0	3.532
.2	3.514
.4	3.4636
.6	3.3903
.8	3.3047
1.0	3.2156
1.6	2.9612
2.0	2.8036
2.6	2.5841
3.0	2.4482
3.6	2.2596
4.0	2.1436
4.6	1.9836
5.0	1.8856
5.6	1.7509
6.0	1.6687
6.6	1.5565
7.0	1.4888
8.0	1.3431
10.0	1.1490
12.320	1.0764
15.0	1.0484
20.0	.9934
25.0	.9384
29.0	.8944

TABLE I.- CENTER-BODY COORDINATES - Continued

(h) $M = 3.03$; 11-inch-diameter sleeve

x, in.	Radius, in.	x, in.	Radius, in.
-9.00	2.750	2.00	4.6417
-8.00	2.880	2.50	4.5485
-7.00	3.100	3.00	4.4935
-6.00	3.450	3.40	4.4920
-5.00	3.860	3.50	4.4912
-4.00	4.280	4.00	4.4872
-3.00	4.680	5.00	4.4792
-2.00	5.000	10.00	4.4392
-1.00	5.220	15.00	4.3992
0	5.3000	20.00	4.3592
.10	5.2906	25.00	4.3192
.20	5.2645	30.00	4.2792
.30	5.2264	35.00	4.2392
.40	5.1828	40.00	4.1992
.45	5.1604	45.00	4.1592
.50	5.1381	50.00	4.1192
.60	5.0944	55.00	4.0792
.70	5.0524	60.00	4.0392
.80	5.0120	65.00	3.9992
.90	4.9731	70.00	3.9572
1.00	4.9358	72.50	4.5000
1.50	4.7711		

TABLE I.- CENTER-BODY COORDINATES - Continued

(1) $M = 3.90$; 8-inch-diameter sleeve

x, in.	Radius, in.	x, in.	Radius, in.
-4.7	2.000	3.75	2.9555
-4.5	2.020	4.00	2.8834
-4.0	2.120	4.50	2.7473
-3.0	2.540	5.00	2.6221
-2.5	2.805	5.50	2.5067
-2.0	3.095	6.00	2.4002
-1.5	3.360	7.00	2.2093
-1.0	3.568	8.00	2.0440
-.8	3.635	9.00	1.8995
-.6	3.690	10.00	1.7734
-.4	3.732	11.00	1.6647
-.2	3.760	12.00	1.5722
0	3.7707	13.00	1.4950
.25	3.7640	14.00	1.4324
.50	3.7430	15.00	1.3838
.75	3.7116	16.00	1.3486
1.00	3.6739	17.00	1.3258
1.25	3.6289	18.00	1.3139
1.50	3.5774	18.782	1.3112
1.75	3.5203	19.00	1.3029
2.00	3.4585	20.00	1.2919
2.25	3.3927	25.00	1.2369
2.50	3.3237	30.00	1.1819
2.75	3.2520	35.00	1.1269
3.00	3.1786	37.50	1.0994
3.25	3.1042	40.50	1.9070
3.50	3.0295		

TABLE I.- CENTER-BODY COORDINATES - Continued

(j) $M = 3.90$; 11-inch-diameter sleeve

x, in.	Radius, in.	x, in.	Radius, in.
-9.0	2.750	9.0	3.3614
-8.0	2.880	10.0	3.2162
-7.0	3.100	11.0	3.0900
-6.0	3.450	12.0	3.9818
-5.0	3.860	13.0	2.8910
-4.0	4.280	14.0	2.8164
-3.0	4.680	15.0	2.7576
-2.0	5.000	16.0	2.7138
-1.0	5.220	17.0	2.6845
0	5.3000	18.0	2.6686
.5	5.2792	18.74	2.6649
1.0	5.2228	20.00	2.6562
1.5	5.1382	25.00	2.6212
2.0	5.0326	30.00	2.5862
2.5	4.9098	35.00	2.5512
3.0	4.7739	40.00	2.5162
3.5	4.6295	45.00	2.4812
4.0	4.4806	50.00	2.4462
4.5	4.3327	55.00	2.4112
5.0	4.1917	60.00	2.3762
6.0	3.9381	65.00	2.3412
7.0	3.7188	69.50	2.3377
8.0	3.5279	72.50	3.000

TABLE I.- CENTER-BODY COORDINATES - Concluded

(k) $M = 5.05$; 11-inch-diameter sleeve

x, in.	Radius, in.
-9.0	3.660
-8.0	4.100
-7.0	4.340
-6.0	4.620
-5.0	4.840
-4.0	5.050
-3.0	5.190
-2.0	5.300
-1.0	5.360
0	5.400
.5	5.3775
1.0	5.3032
1.5	5.1569
1.6	5.1176
1.7	5.0763
1.8	5.0342
1.9	4.9917
2.0	4.9492
2.1	4.9068
2.2	4.8648
3.0	4.5464
5.0	3.8704
7.0	3.3310
9.0	2.8910
11.0	2.5274
13.0	2.2294
15.0	1.9980
17.0	1.8330
19.0	1.7360
20.440	1.7140
25.000	1.6684
30.000	1.6184
40.000	1.5184
50.000	1.4184
60.000	1.3184
70.000	1.2184

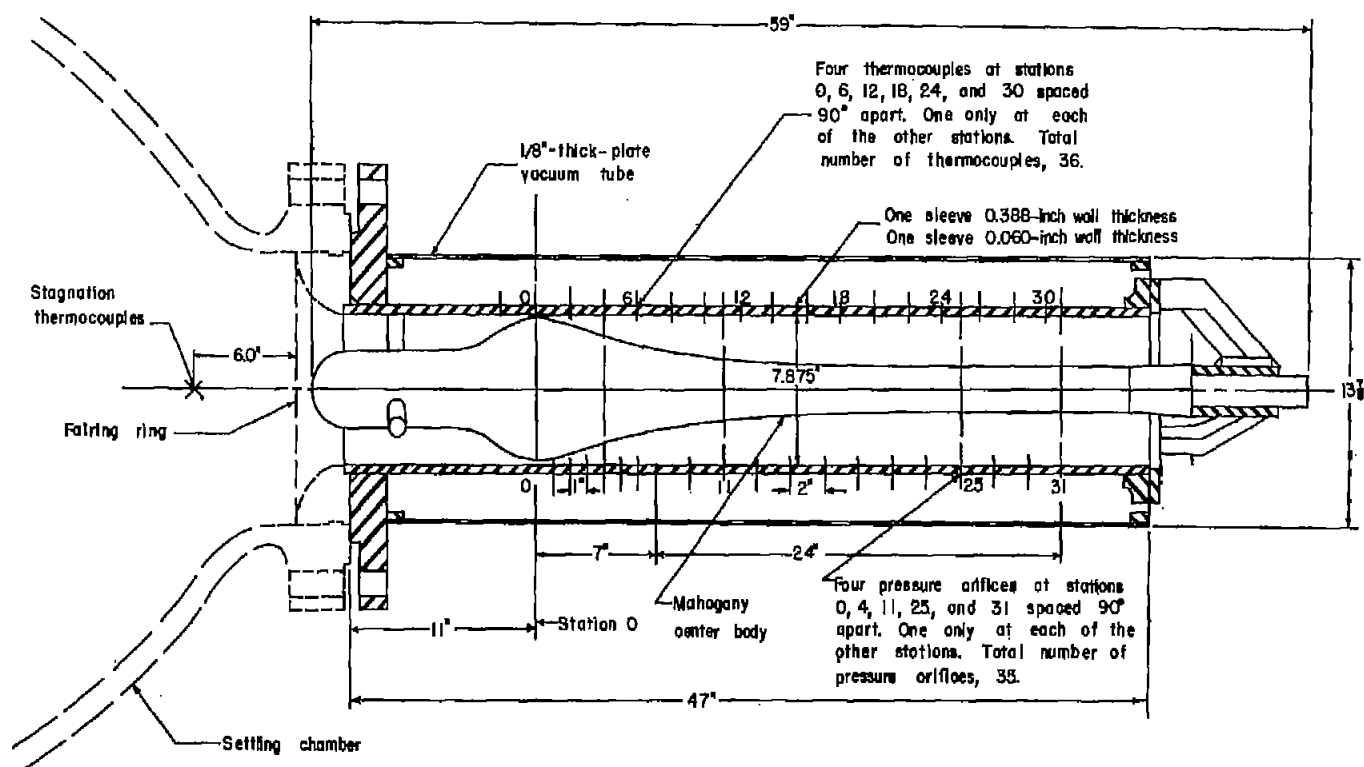
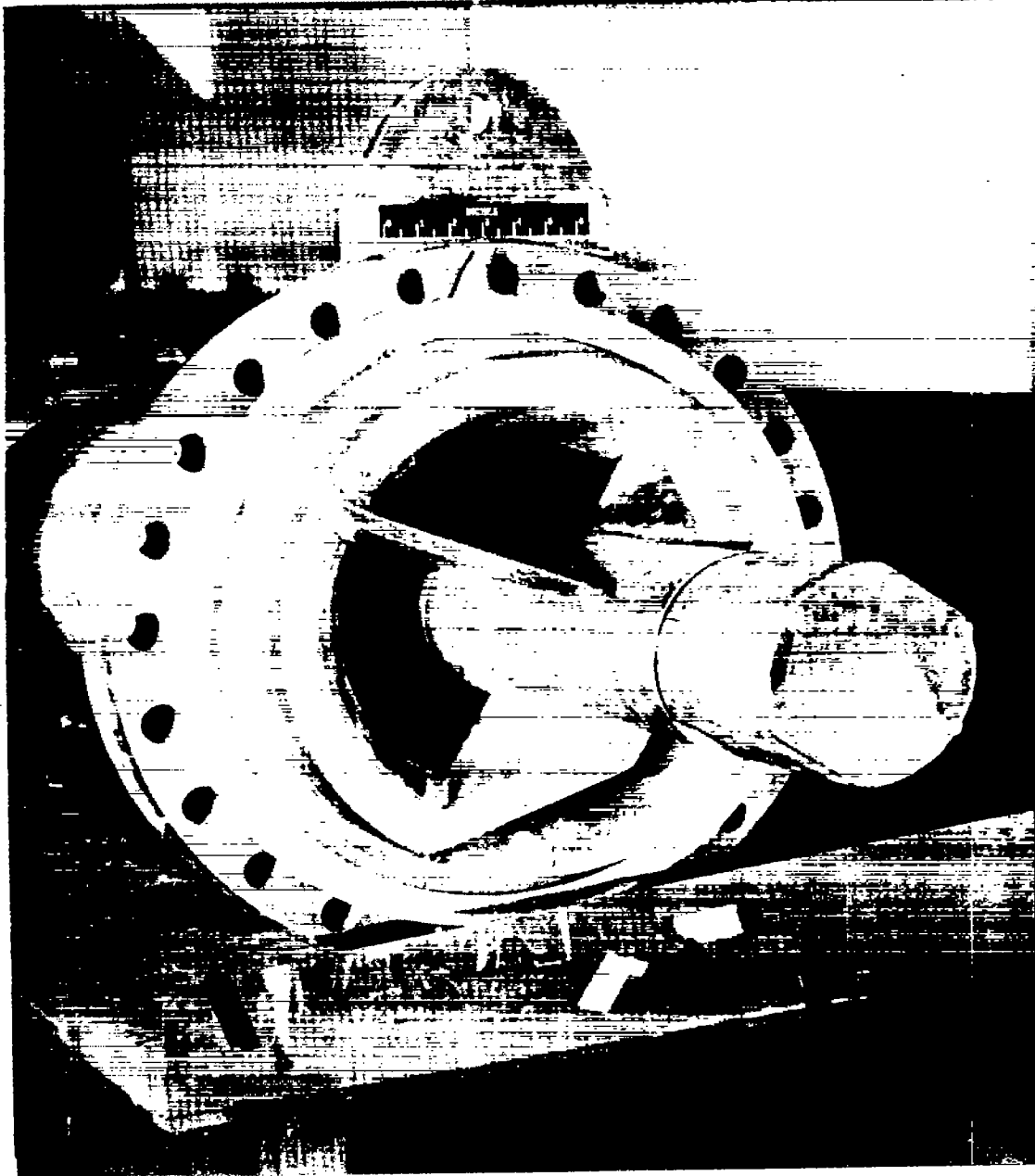


Figure 1.- Test arrangement. Dimensions are in inches.



L-57-2671
Figure 2.- Inlet and center-body support for 11-inch sleeve.

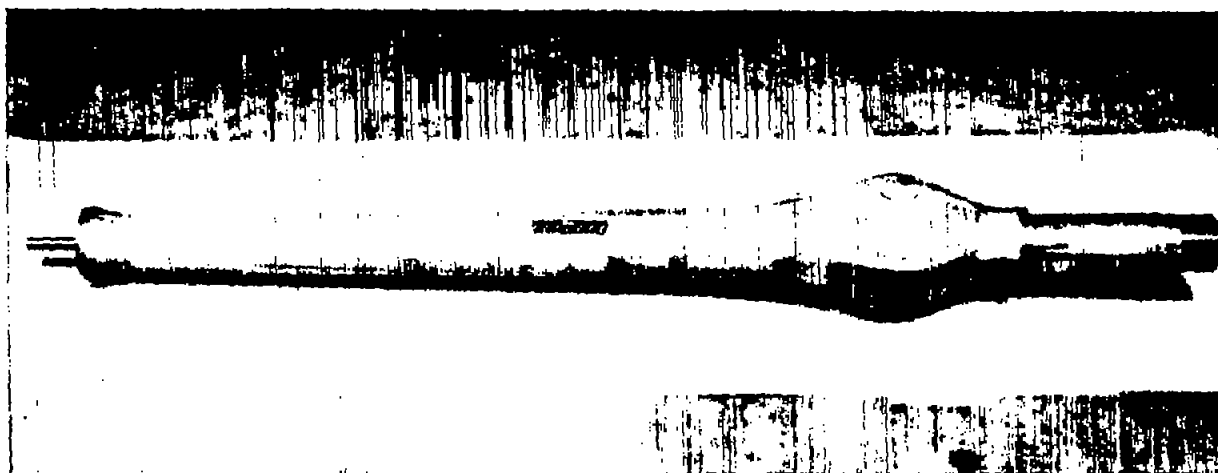


Figure 3.- Typical center body. L-57-2670

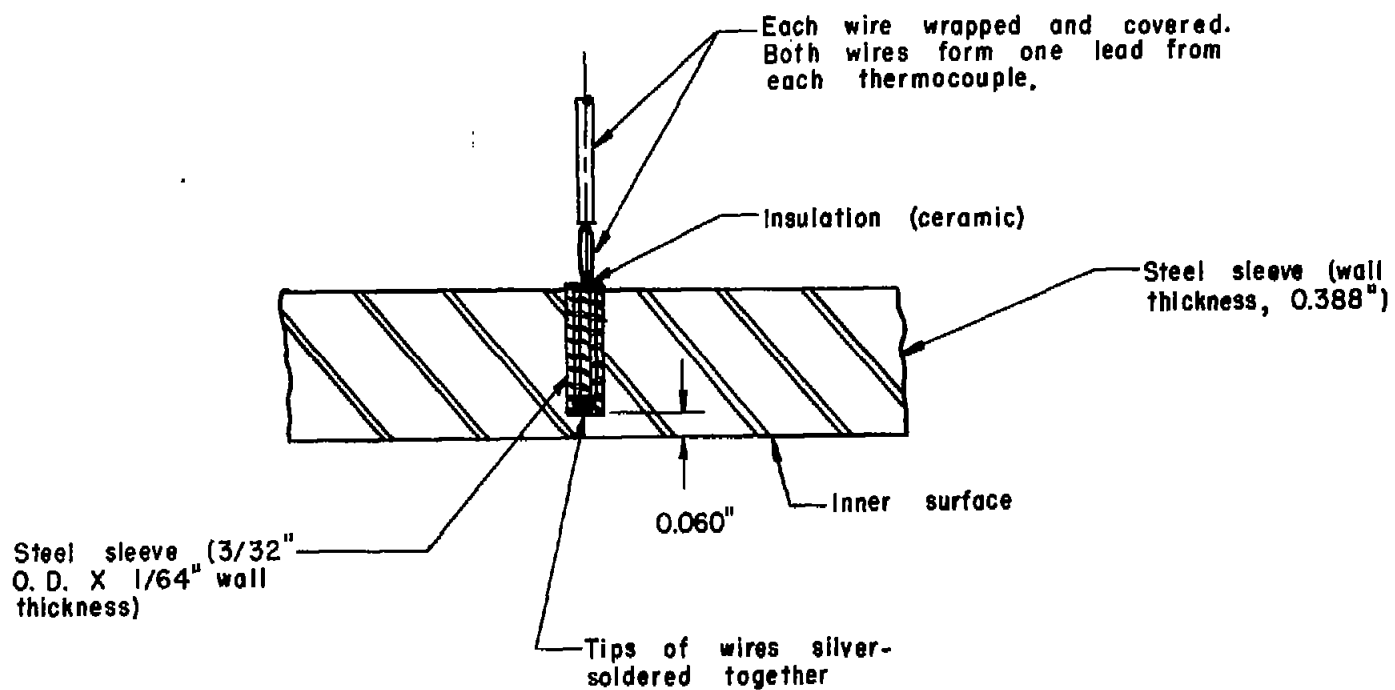


Figure 4.- Thermocouple installation.

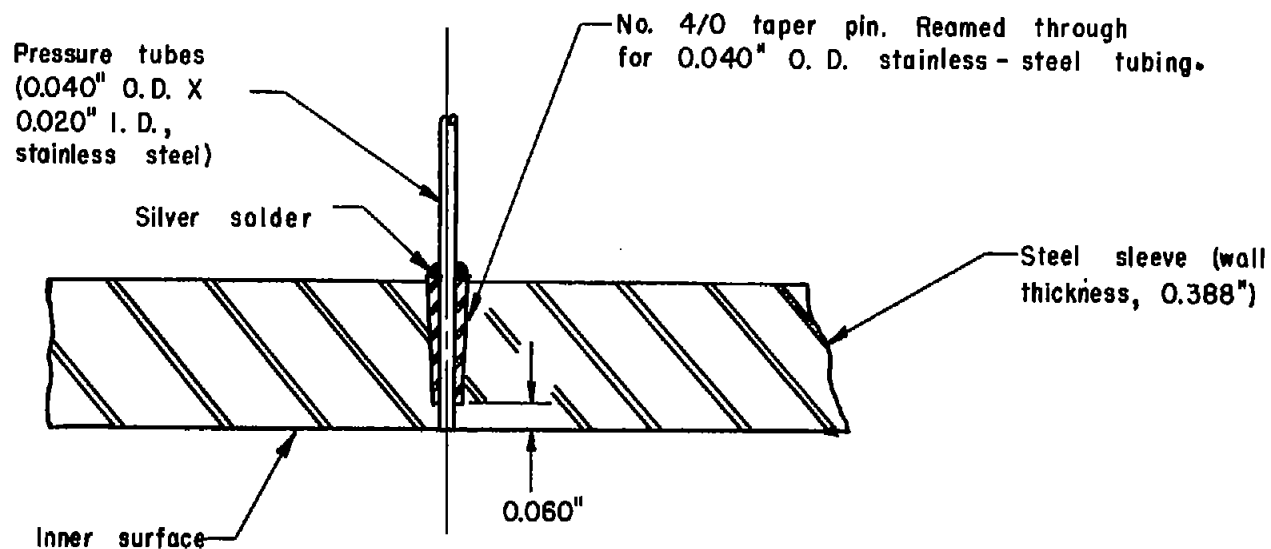


Figure 5.- Static-pressure-orifice installation.

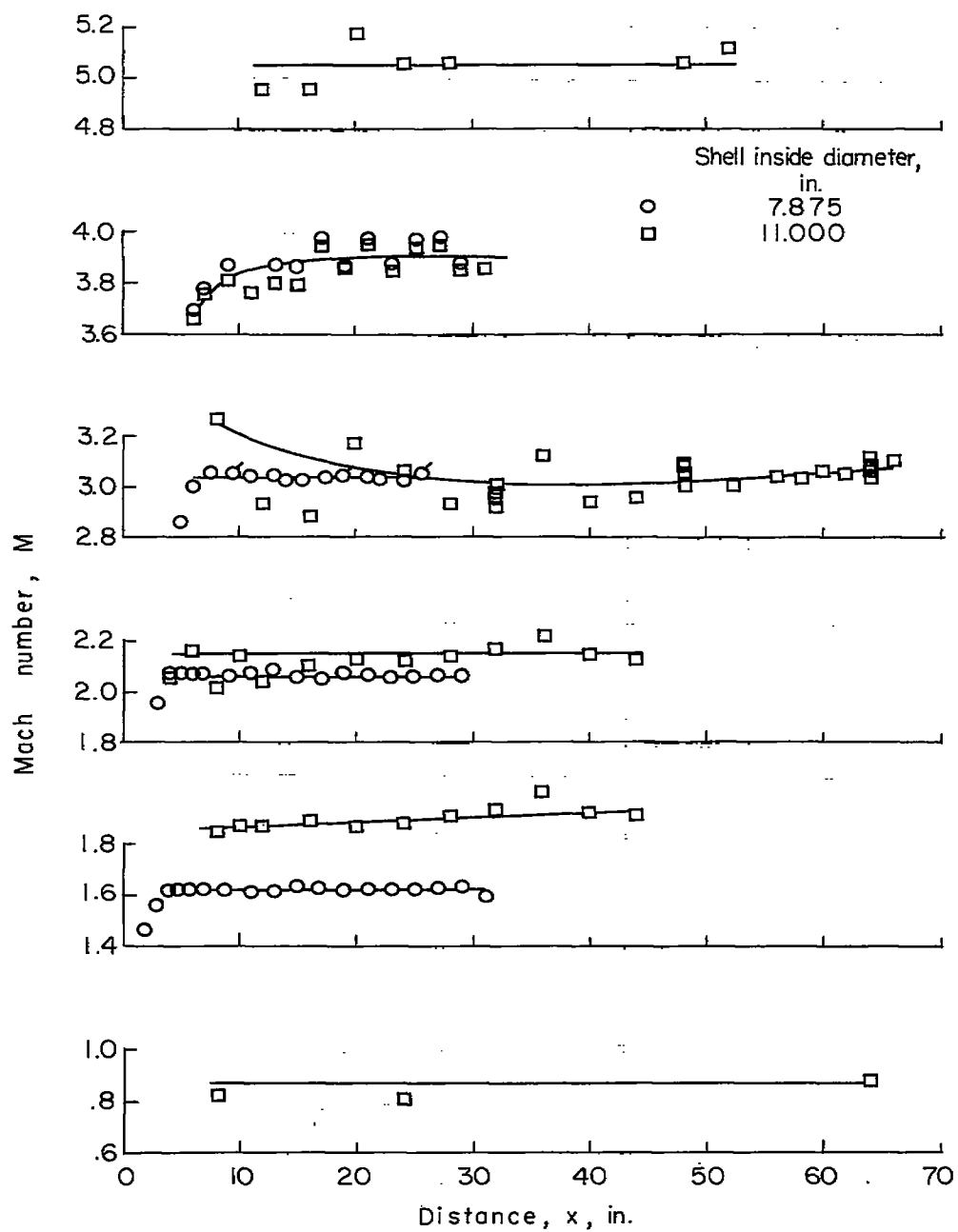


Figure 6.- Mach number distribution.

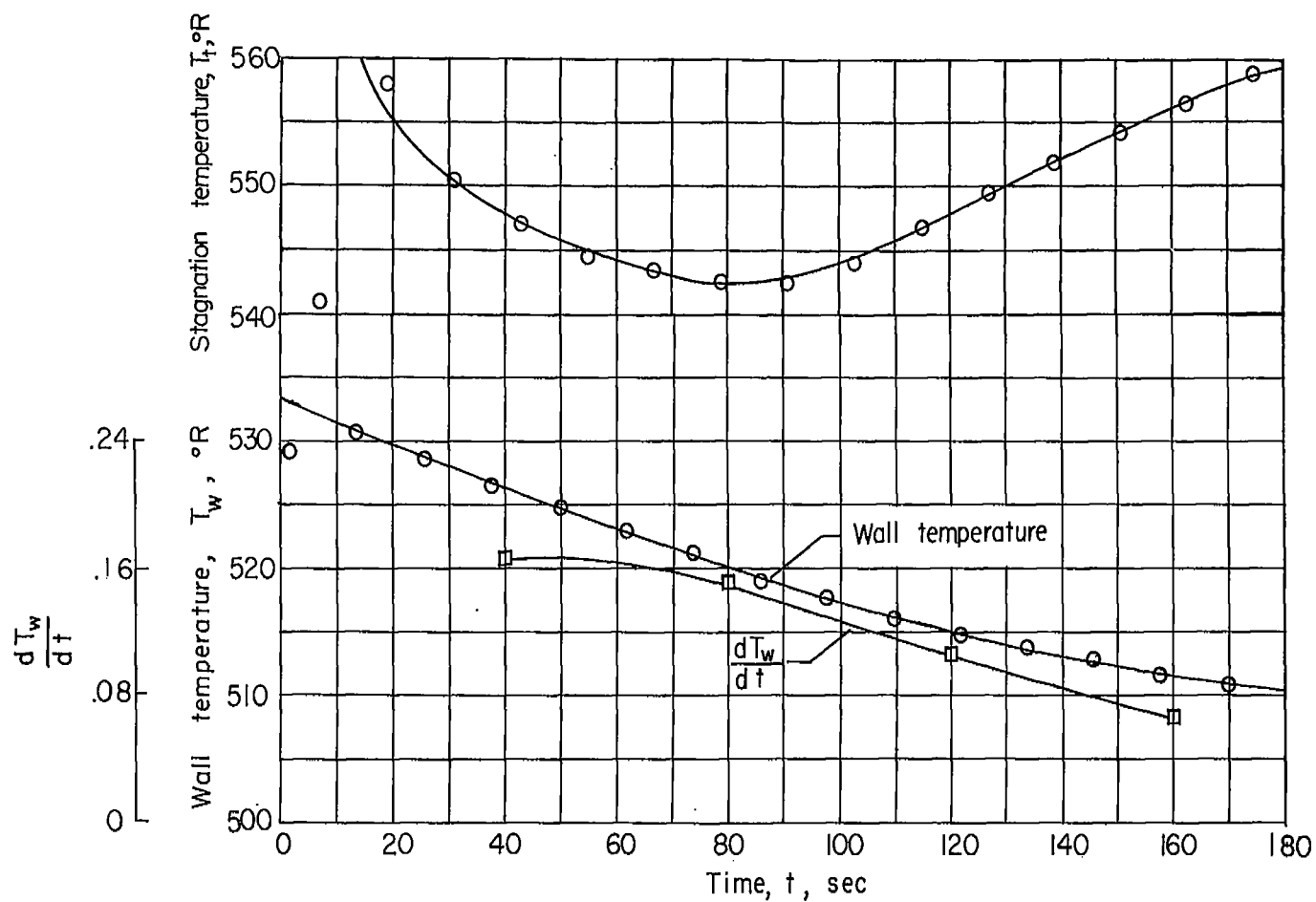


Figure 7.- Variation of stagnation temperature, wall temperature at station 14, and slope $\frac{dT_w}{dt}$ with time for 11-inch nozzle at $M = 3.90$ and $p_0 = 353$ lb/sq in. gage.

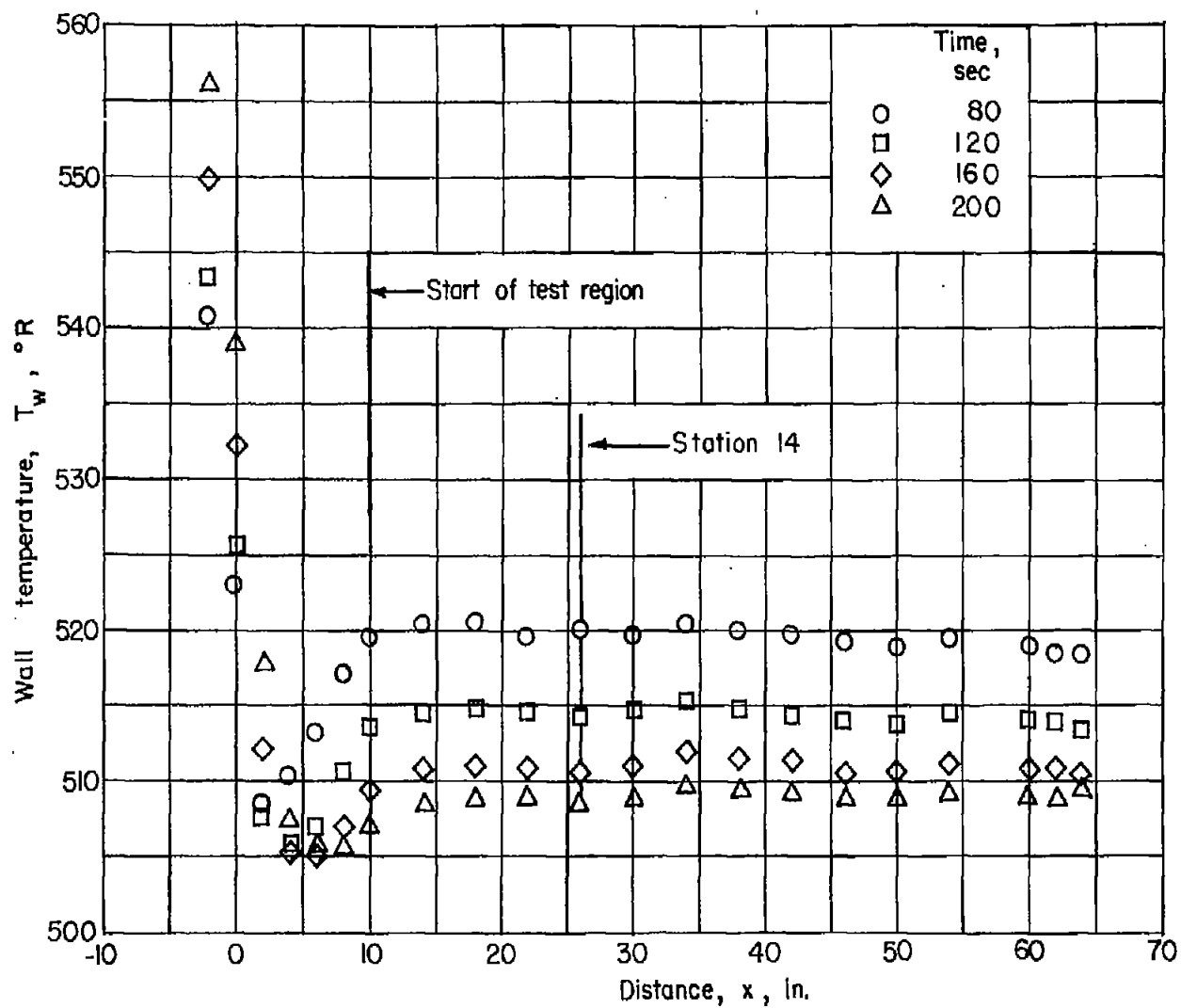


Figure 8.- Variation of wall temperature with longitudinal distance for $M = 3.90$ and $P_0 = 353$ lb/sq in. gage.

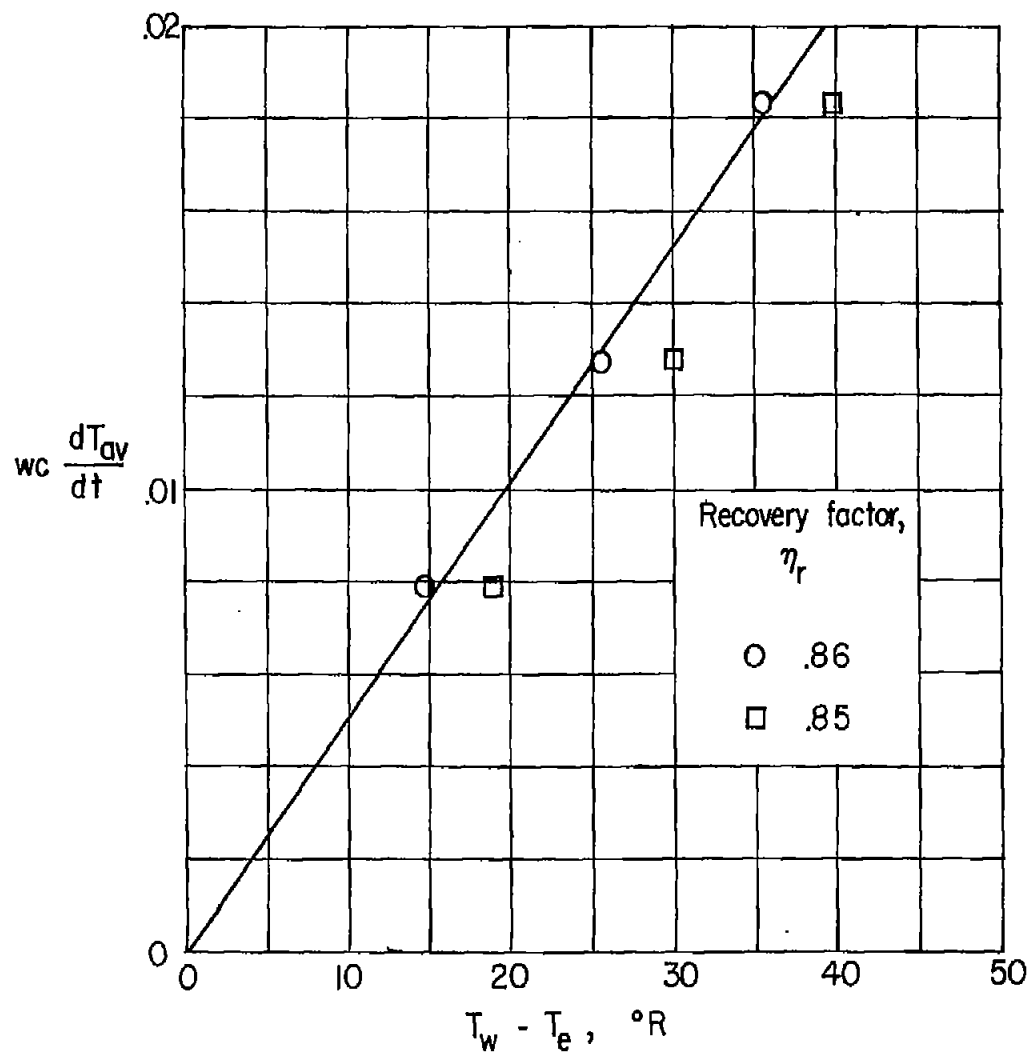


Figure 9.- Heat input as a function of recovery factor and $T_w - T_e$ at station 14 for $M = 3.90$ and $P_0 = 353$ lb/sq in. gage.

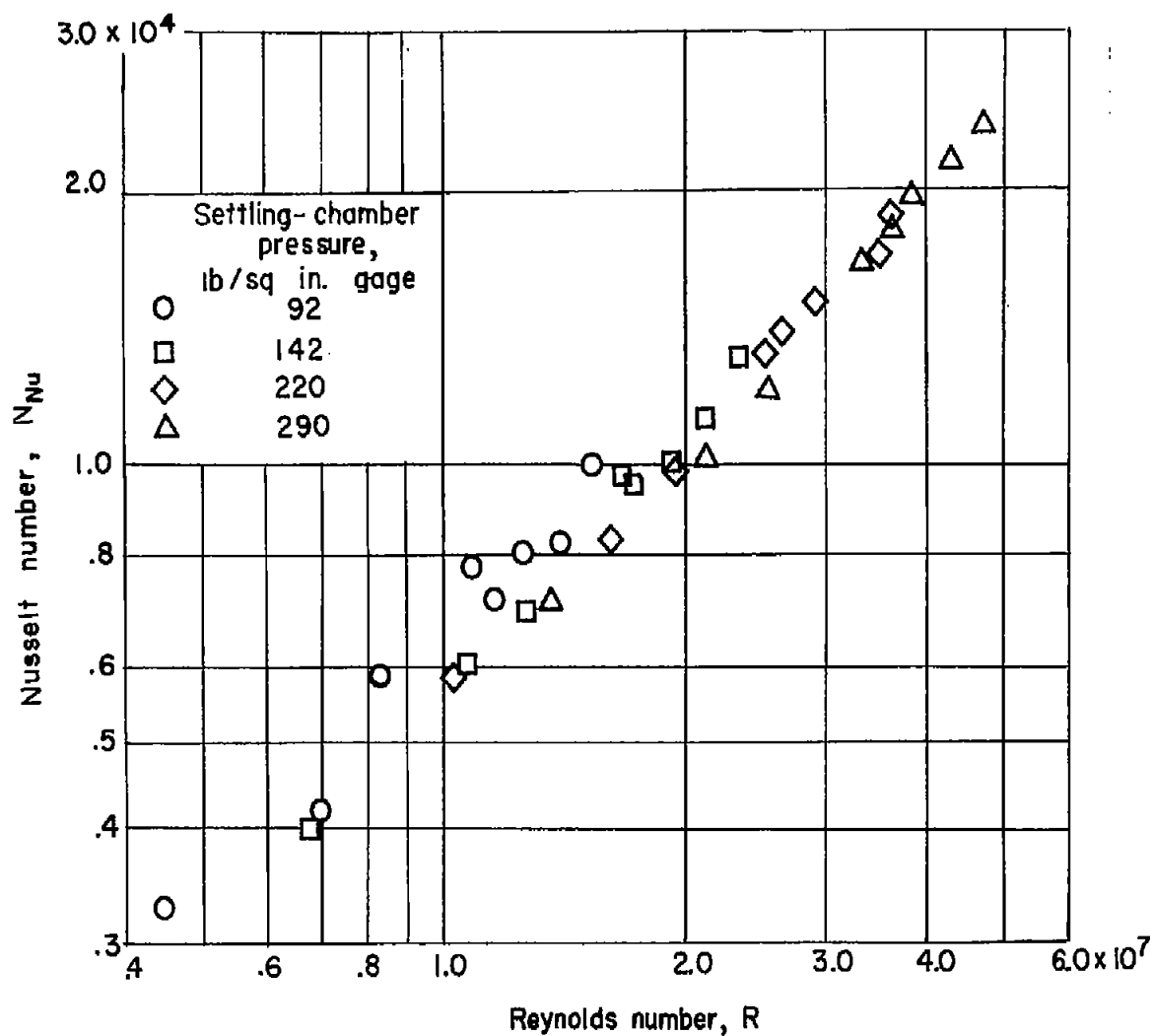
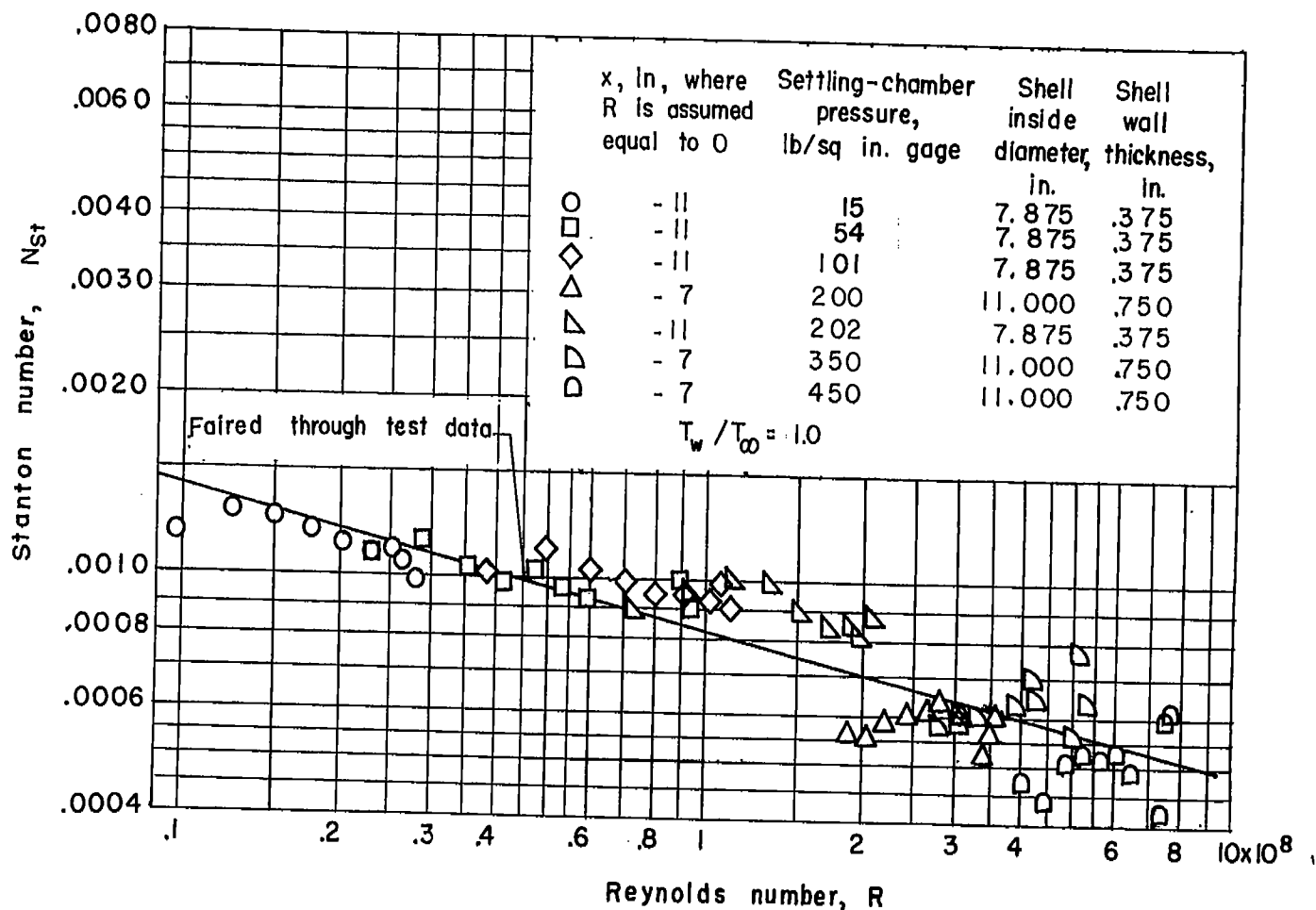
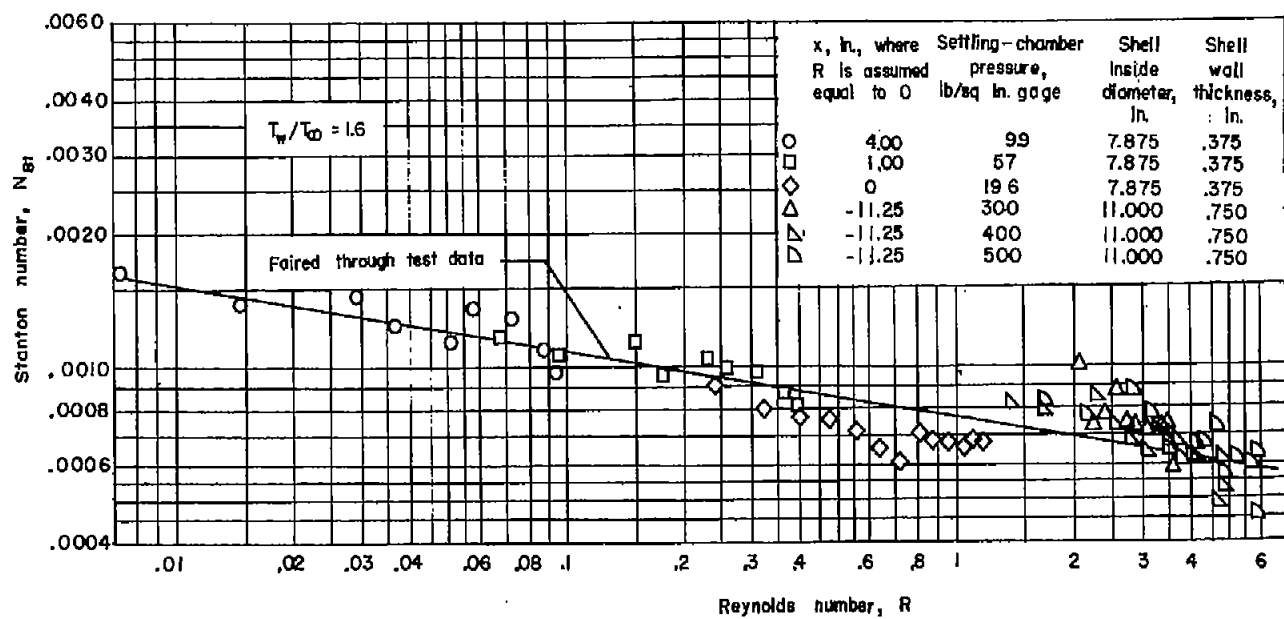


Figure 10.- Variation of local Nusselt number with local Reynolds number for $x = 0$ at station 0 for $M = 3.03$.



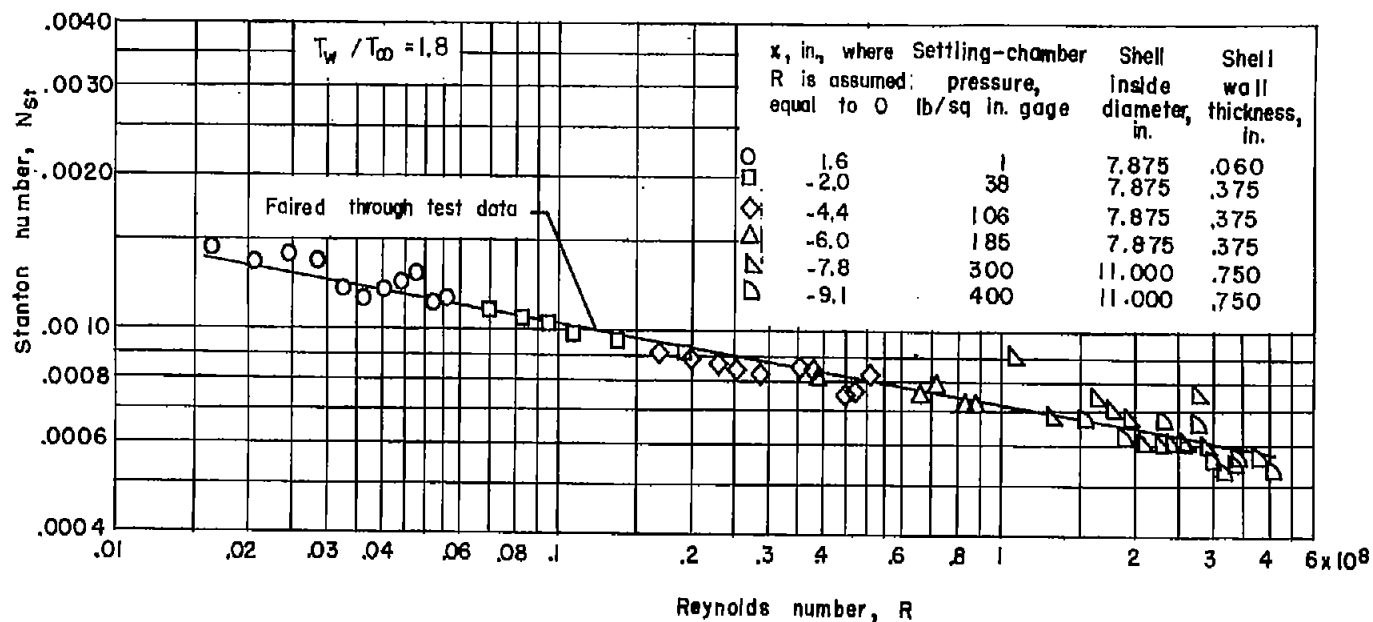
(a) $M = 0.87$.

Figure 11.- Variation of local Stanton number with Reynolds number for corrected location of $x = 0$. Viscosity determined for wall temperature.



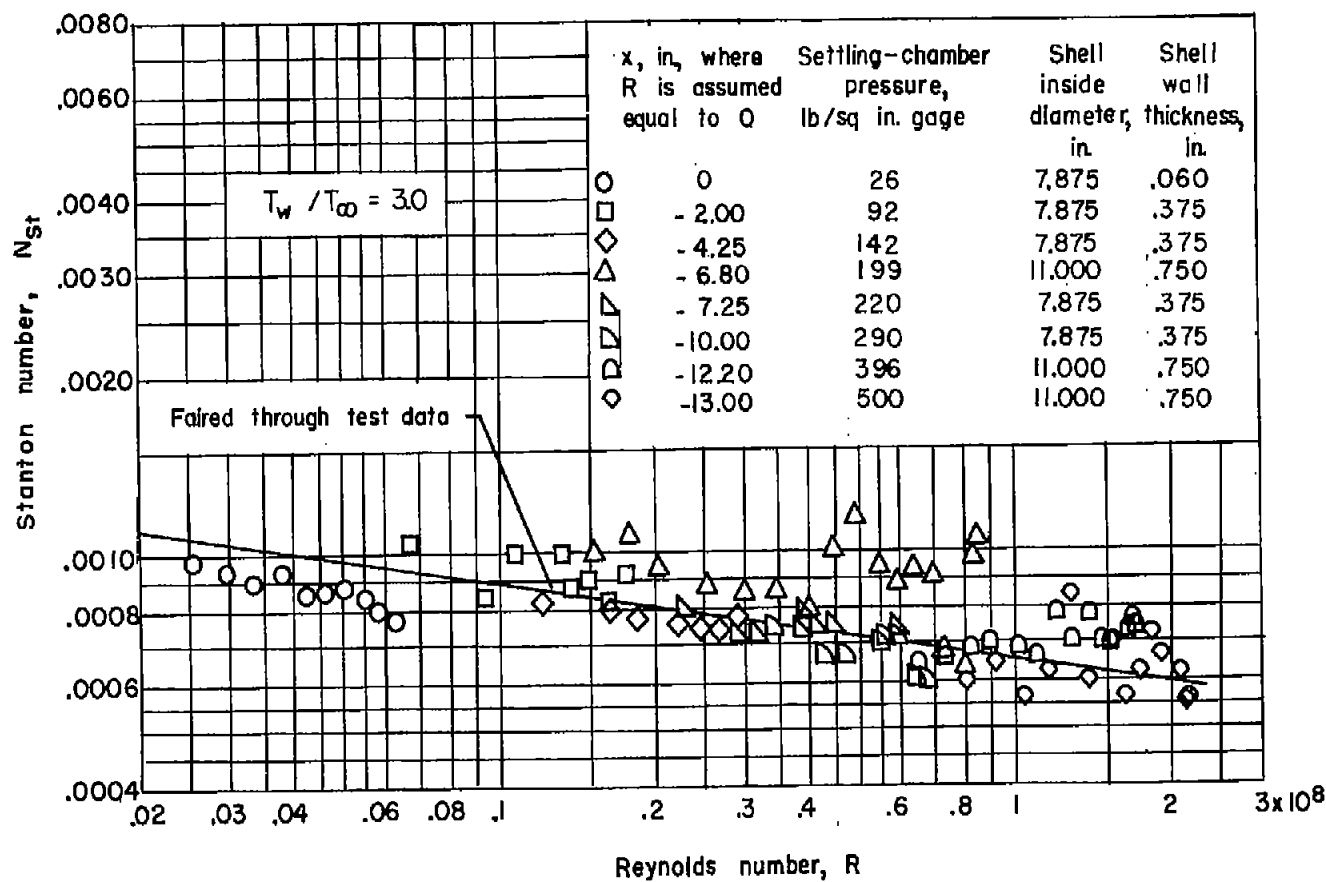
(b) $M = 1.62$.

Figure 11.- Continued.



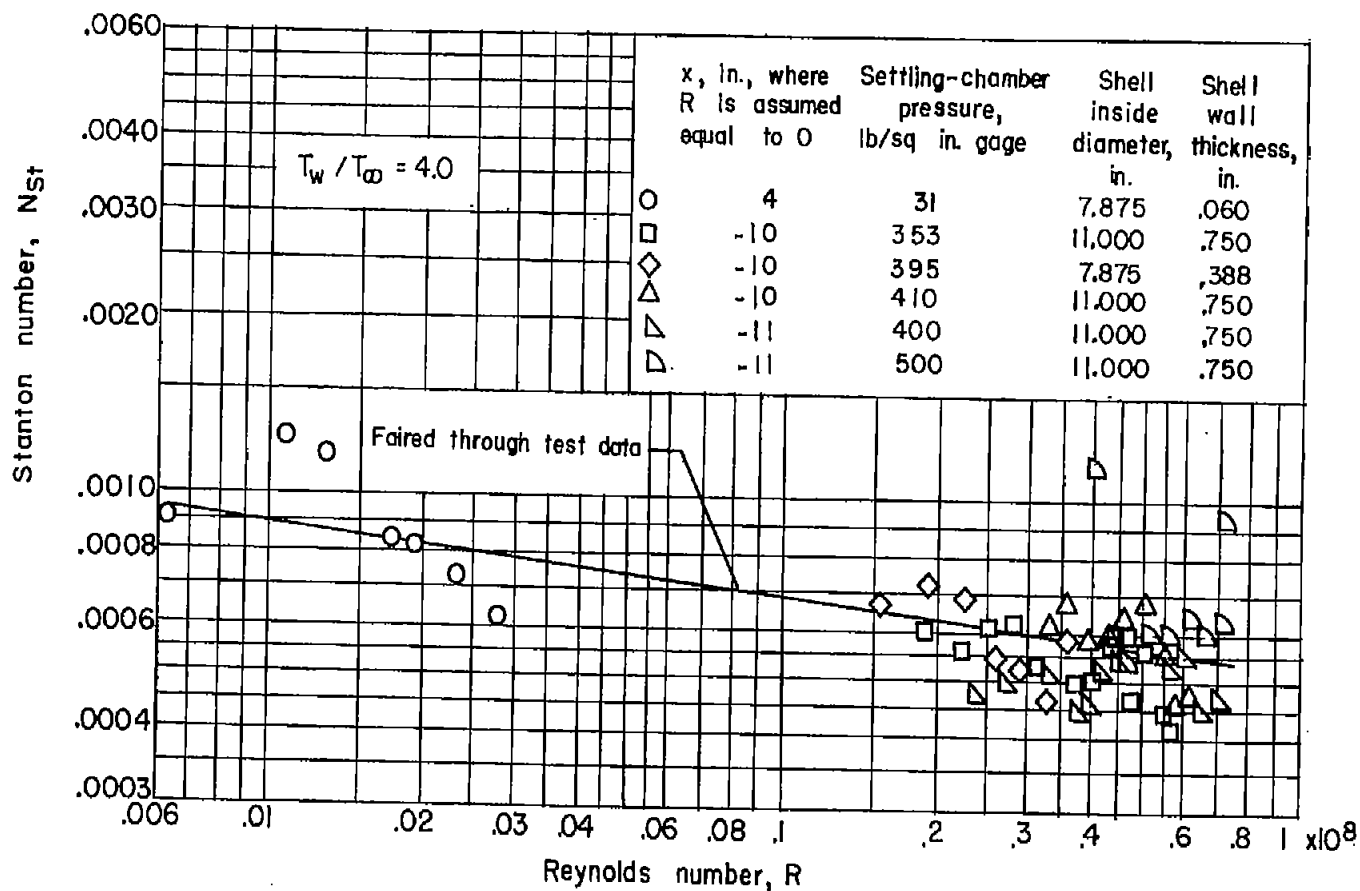
(c) $M = 2.06$.

Figure 11.- Continued.



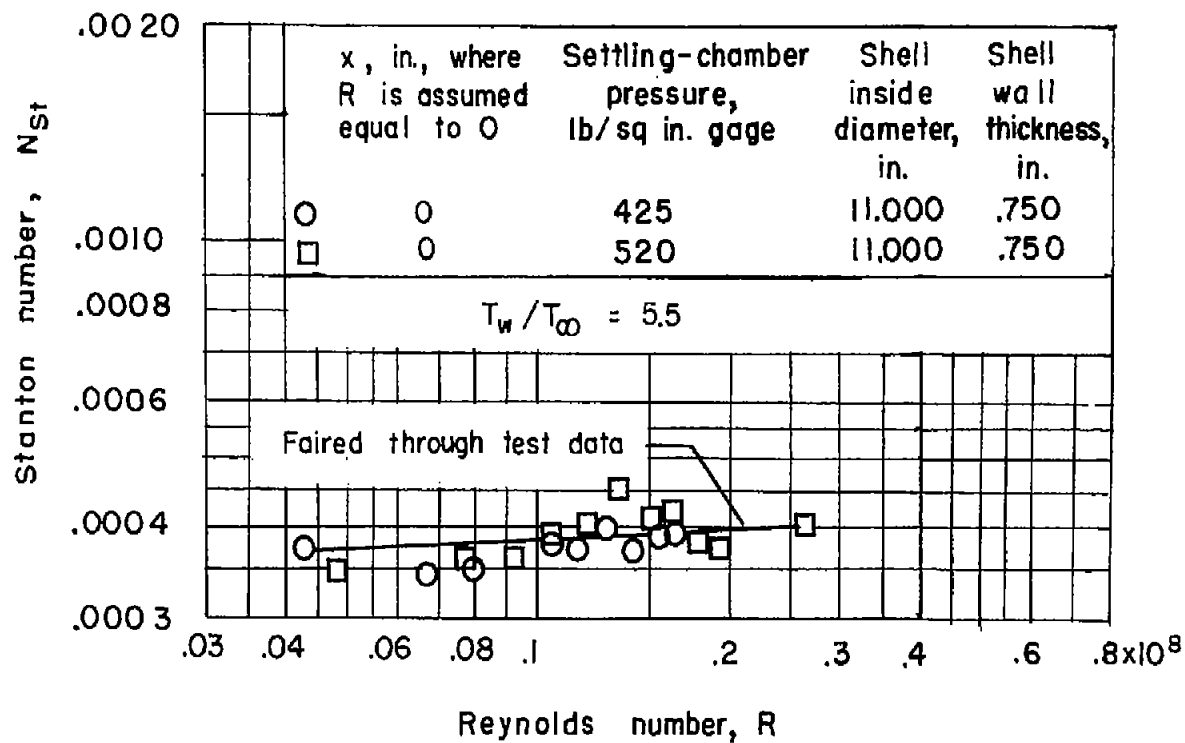
(d) $M = 3.03$.

Figure 11.- Continued.



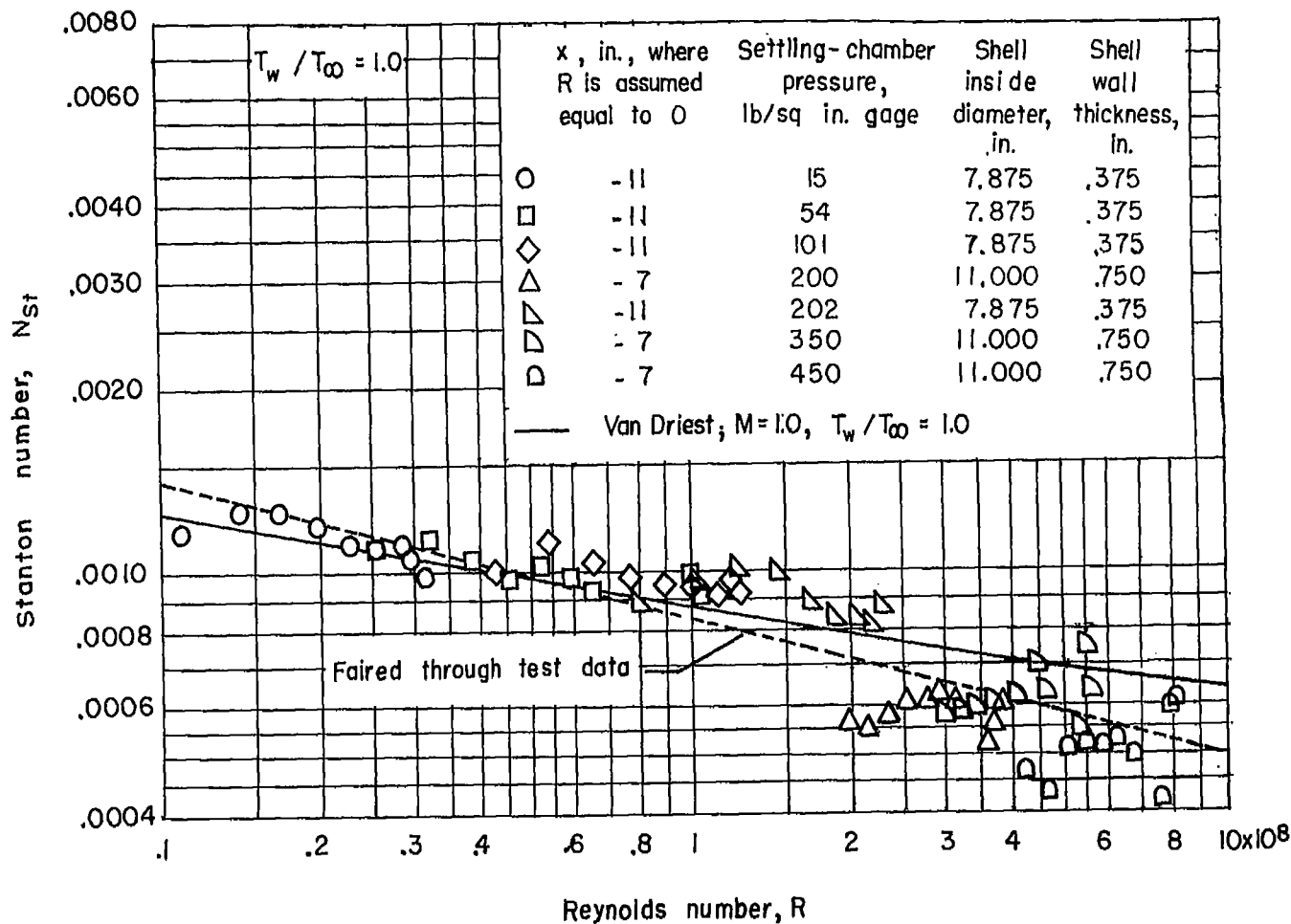
(e) $M = 3.90$.

Figure 11.- Continued.



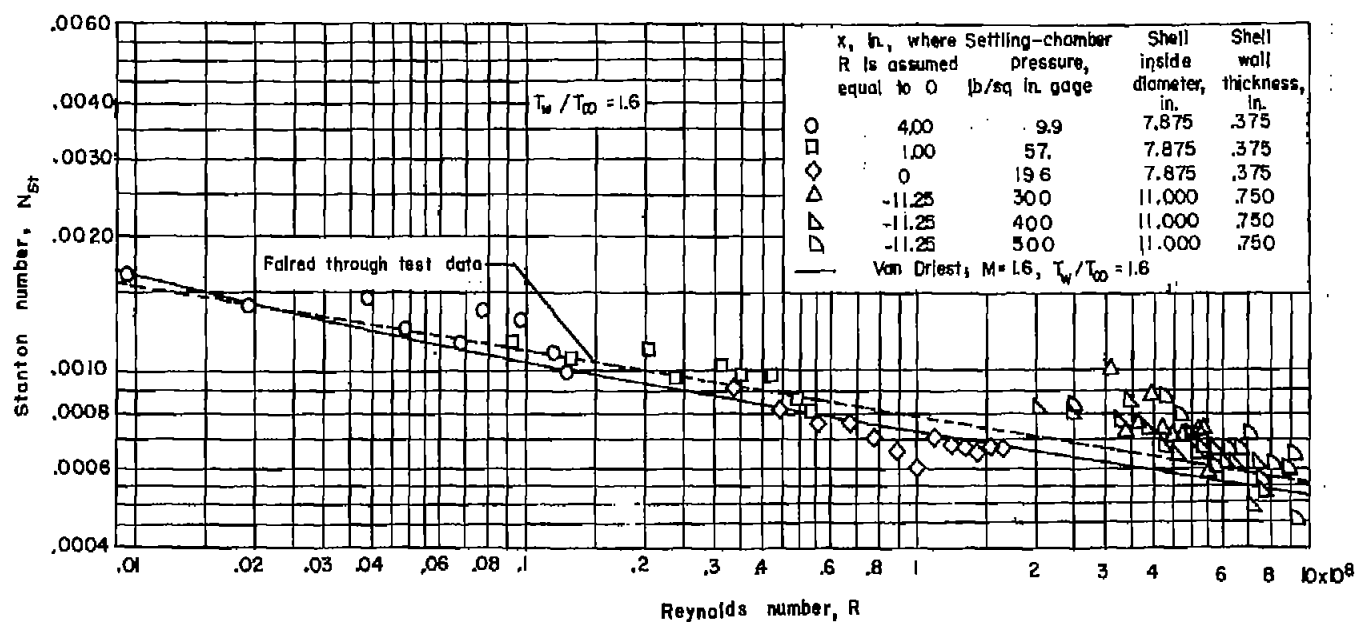
(f) $M = 5.05$.

Figure 11.- Concluded.



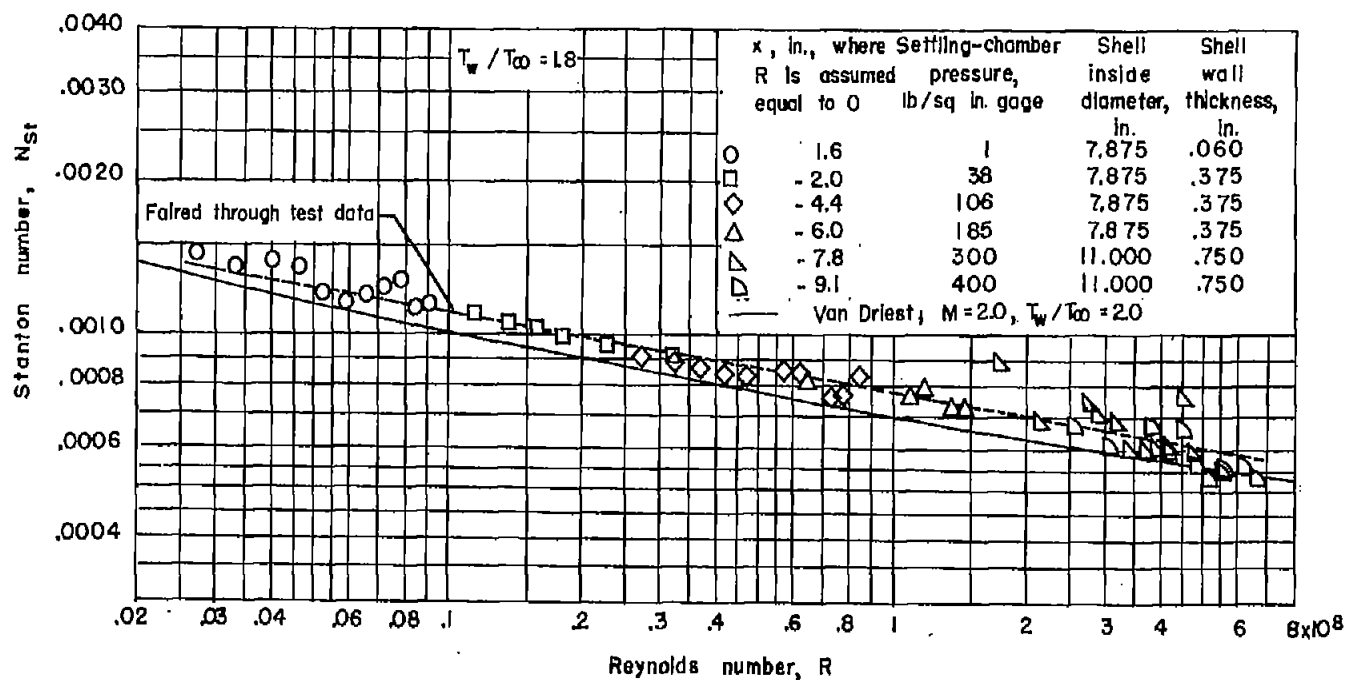
(a) $M = 0.87$.

Figure 12.- Variation of local Stanton number with Reynolds number for corrected location of $x = 0$. Viscosity determined at free-stream temperature.



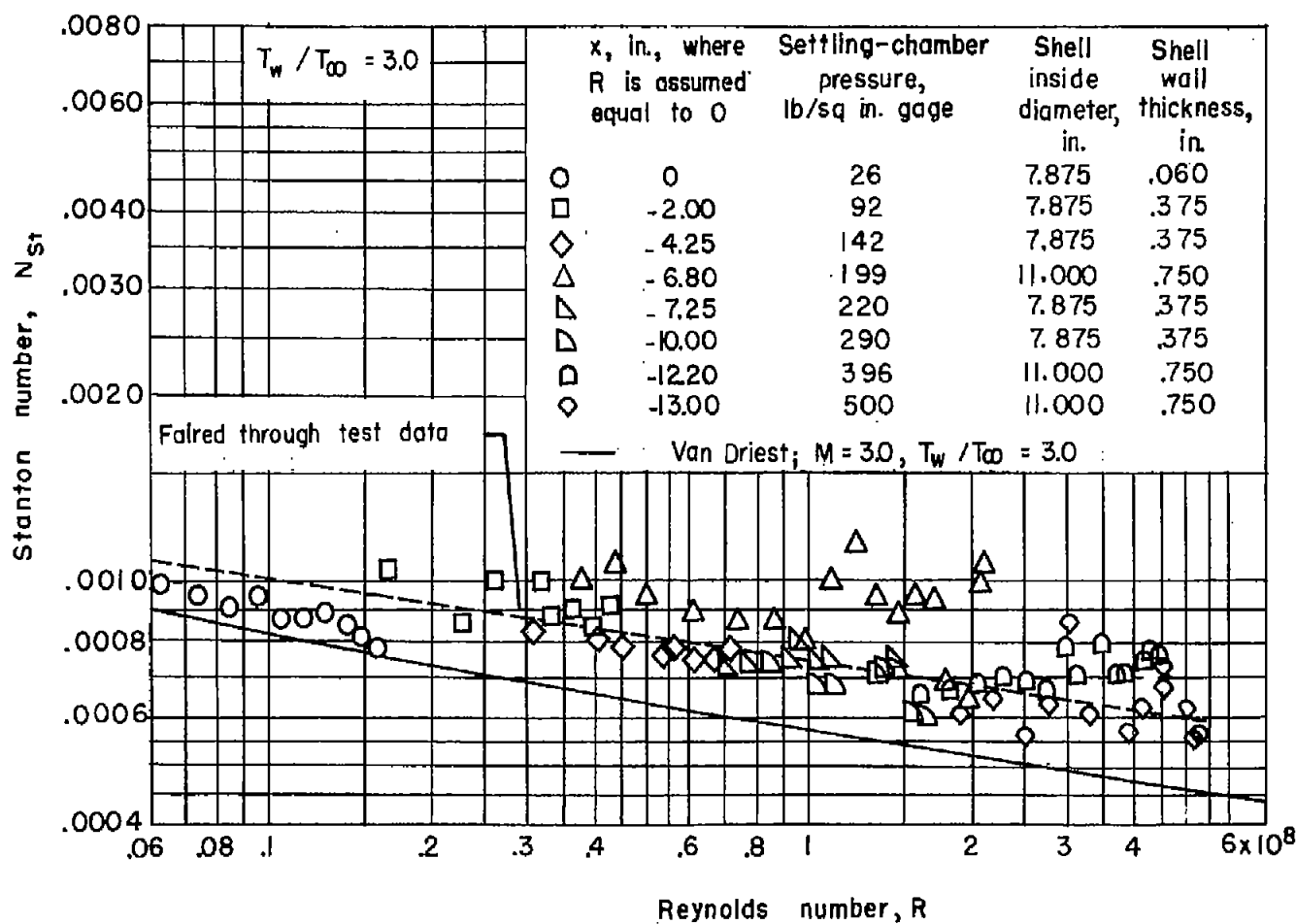
(b) $M = 1.62$.

Figure 12.- Continued.



(c) $M = 2.06$.

Figure 12.- Continued.



(d) $M = 3.03$.

Figure 12.- Continued.

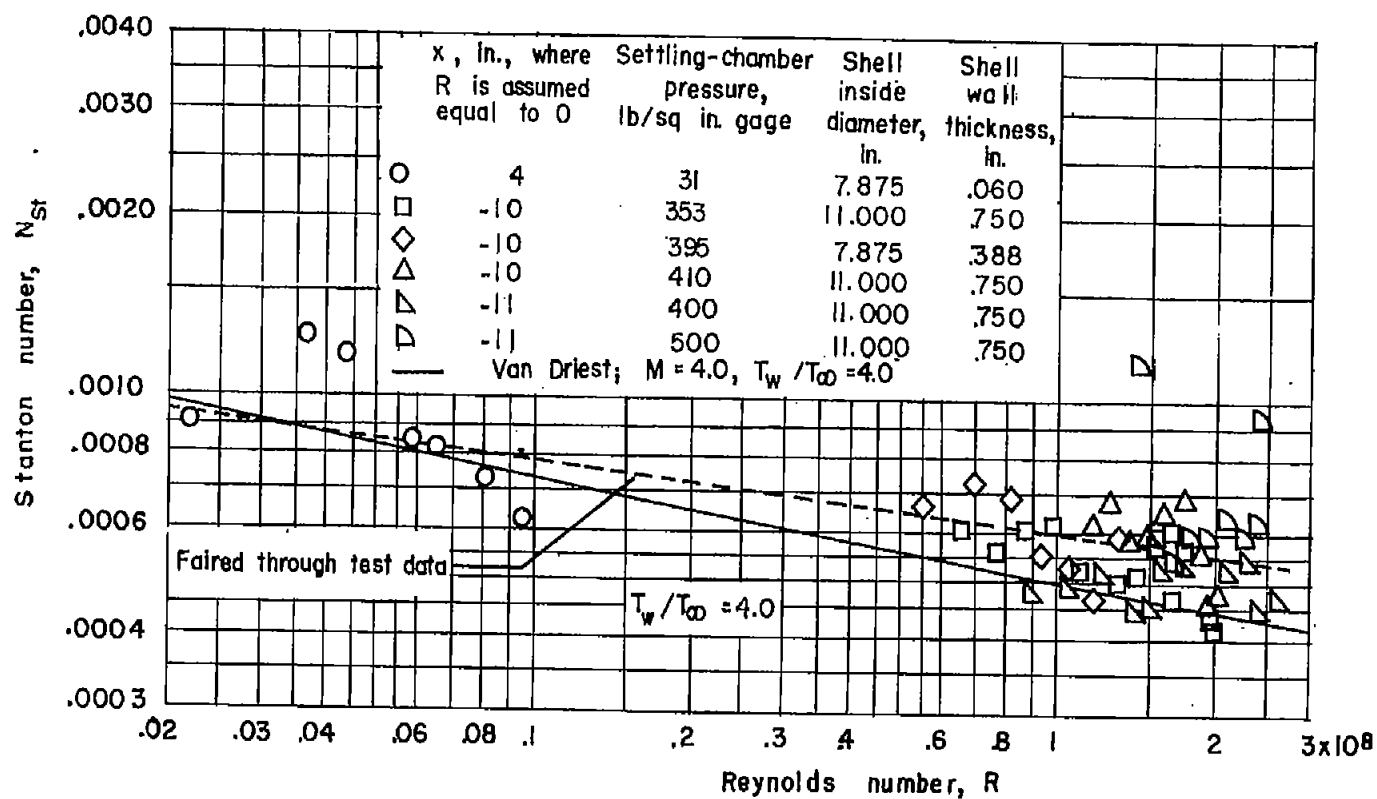
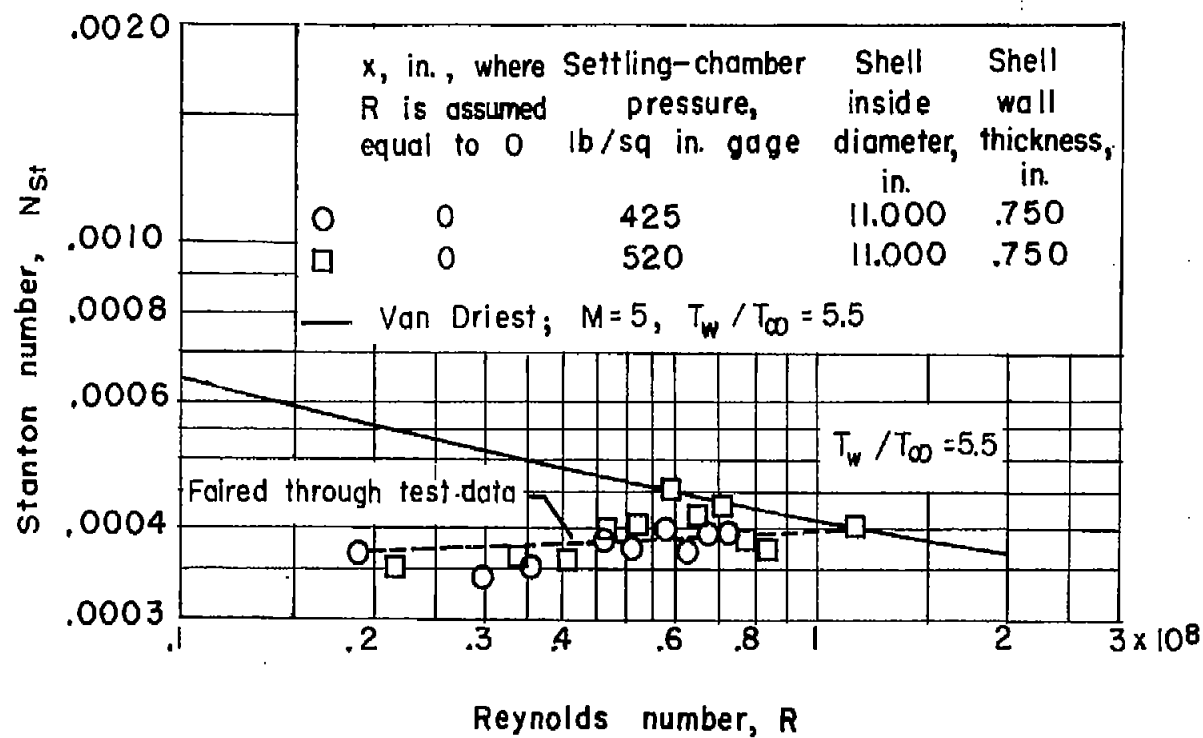
(e) $M = 3.90$.

Figure 12.- Continued.



(f) $M = 5.05$.

Figure 12.- Concluded.

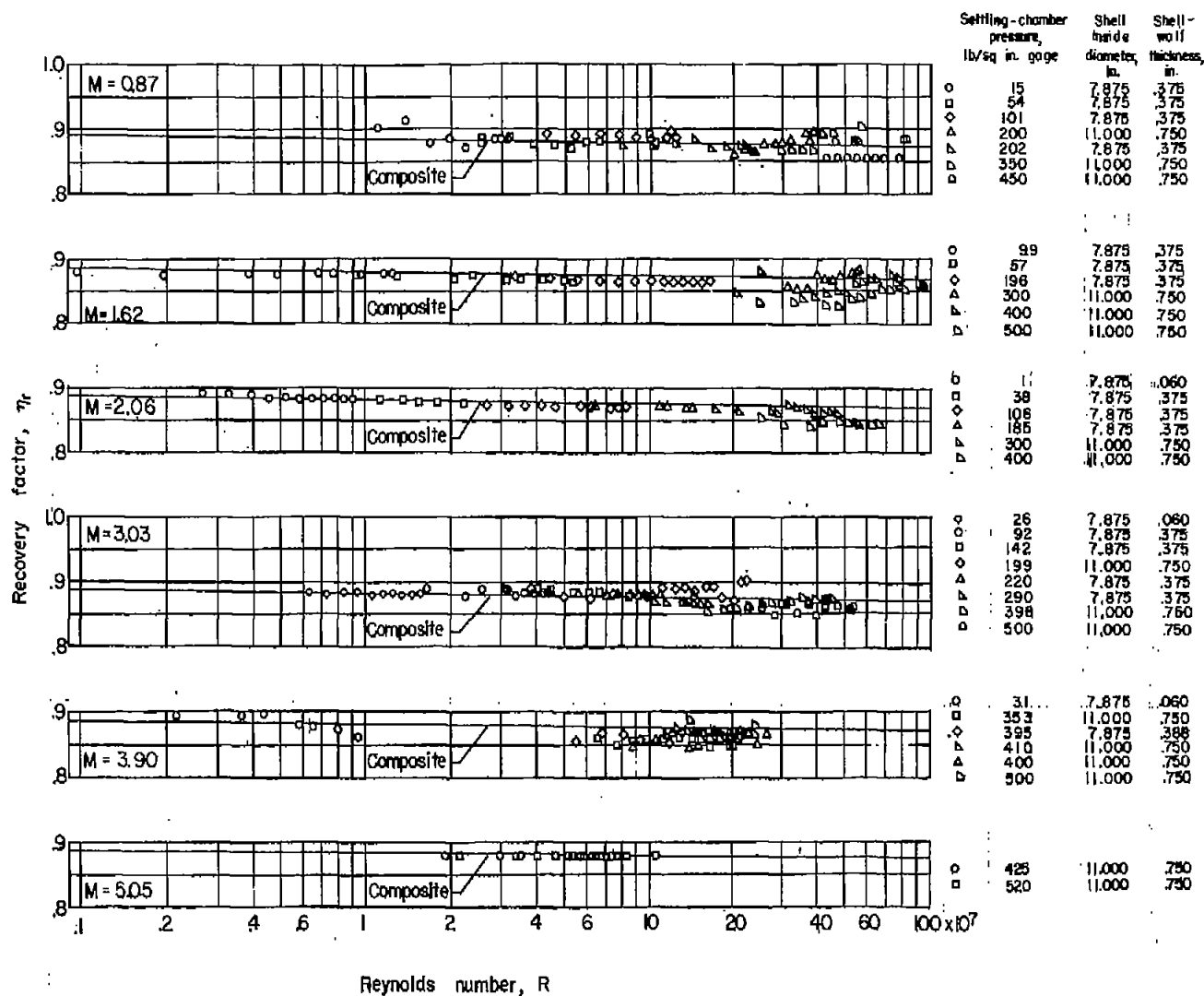


Figure 14.- Variation of recovery factor with Reynolds number for corrected location of $x = 0$.
Viscosity determined for free-stream temperature.

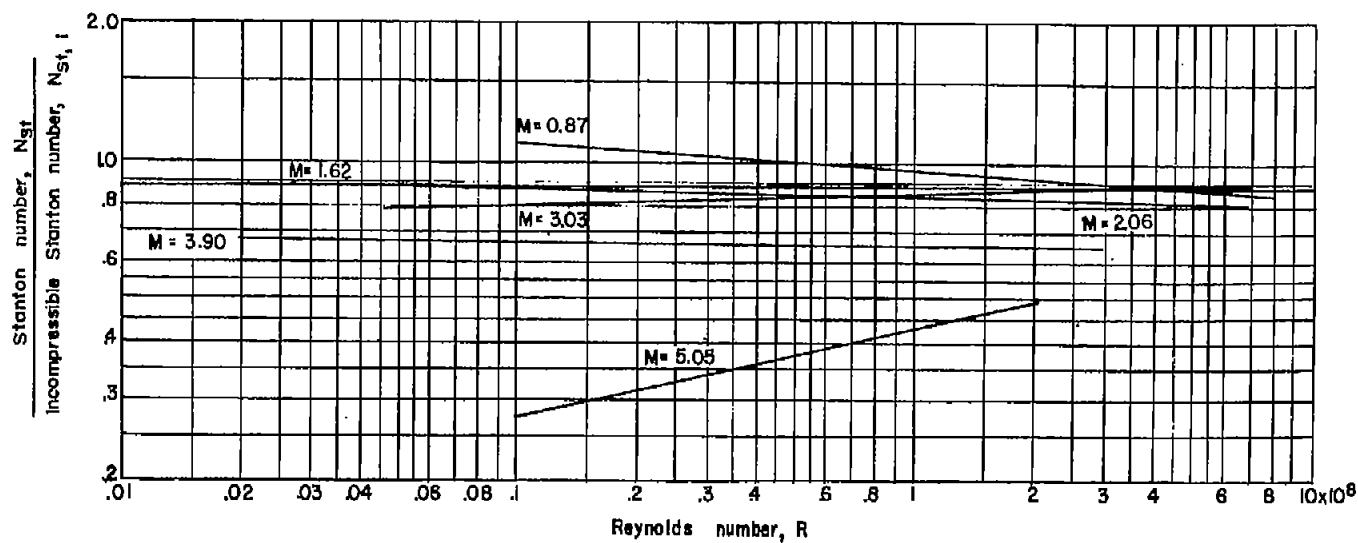


Figure 15.- Variation with Reynolds number of ratio of test Stanton number to incompressible Stanton number.